

# UC Irvine

## UC Irvine Previously Published Works

### Title

Cell damage by near-IR microbeams

### Permalink

<https://escholarship.org/uc/item/68c807j8>

### Journal

Nature, 377(6544)

### ISSN

0028-0836

### Authors

König, K  
Liang, H  
Berns, MW  
[et al.](#)

### Publication Date

1995-09-01

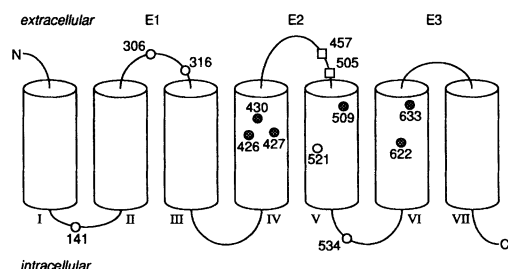
### DOI

10.1038/377020a0

### Copyright Information

This work is made available under the terms of a Creative Commons Attribution License, available at <https://creativecommons.org/licenses/by/4.0/>

Peer reviewed



Correlated mutations in rat olfactory receptors (see also ref. 7). Transmembrane  $\alpha$ -helices (denoted by roman numerals) are shown as cylinders, interhelical loops as lines. E1, E2 and E3 indicate respective extracellular loops. Squares indicate correlated E2 residues; shaded circles indicate predicted ligand-binding residues; open circles indicate correlated residues of unknown function.

Correlated residues	$r_{ij}$	
316	457	0.973
430	457	0.973
505	509	0.997

Significant pairwise correlations with E2 residues.  $r_{ij}$  is the correlation coefficient for pairwise comparison of sequence positions  $i$  and  $j$ . Correlations were calculated by the CORMUT option of WHATIF<sup>15</sup>.

The potential importance of loop E2 has already been suggested by the finding of nonrandom amino-acid substitutions resulting from positive selection<sup>10</sup>, implying that loop E2 has a function unique to each receptor subtype. Also, a survey of the olfactory receptor family by hydrophobicity profiles<sup>11</sup> has shown that loop E2 contains approximately 35 residues, substantially more than most other members of the G-protein-coupled receptor superfamily.

Among possible functions for loop E2, interactions with odour molecules seem less likely because the hydrophilic loop and aqueous environment provide a poor binding site for odour molecules, which for terrestrial mammals are typically hydrophobic<sup>2</sup>. Interactions with odour binding proteins (OBPs) or chaperonins are also less likely because they appear inconsistent with the extreme sequence diversity in the loop and the apparent functional specificity of each subtype (see ref. 10).

A more likely possibility is raised by the

recent finding that messenger RNA for putative olfactory receptors is present in the axon terminals of ORNs within their target glomerulus<sup>5,6</sup>, suggesting that the receptor molecules may be involved in guiding axons to their target glomeruli. We propose that loop E2 contributes to this through axon-to-axon or axon-to-substrate interactions. Sequence motifs in the loop, especially conserved cysteines, may mediate this function; similar motifs are present in integrins and growth factors.

The correlated mutation analysis<sup>7</sup> shows a one-to-one correspondence between the residues at positions 457 (loop E2) and 430 (predicted odour binding site; see table in figure legend). Thus, the residue at position 457 carries sufficient information to infer the residue at position 430 (Lys:His, Gln:Gln, Asn:Lys and Val:Ile, respectively). Positions 505 and 509 form another such pair. We anticipate that additional correlated pairs will be revealed by analysis of further receptors. Loop E2 can therefore function as a cell-surface identifier for the receptor subtype, reflecting the specificity of the odour-binding pocket. Consistent with this is our observation that no two olfactory receptor subtypes share the same loop E2 sequence<sup>12,13</sup>.

The variation of loop E2 residues across

subtypes may contribute to the abilities of ORN axons of one subset to find their common target glomerulus, and of related subsets to target neighbouring glomeruli. This could provide a basis for the functional topography of the olfactory bulb. The loops could form homophilic interactions between axons, or bind preferentially to specific receptors, adhesion, or chemotactic molecules. Other extracellular domains (E1 and E3) could participate in these interactions, but they do not seem to share the special properties of loop E2, namely the hypervariability, positive selection, uncommon length and cysteine motifs.

Immunocytochemistry has suggested the presence of the olfactory receptor protein in the ORN axons (R. Reed, personal communication). Furthermore, receptor mRNA is evident in ORNs before their axons reach the olfactory bulb and establish synapses<sup>14</sup>, consistent with a role for the receptor in development.

Olfactory receptors may perform a dual role, as odour receptors in the sensory cilia and as guidance molecules in the axons. This may represent a more highly specific mechanism of axon guidance than any previously identified and implies a novel property for some members of the G-protein-coupled receptor superfamily.

**Michael S. Singer, Gordon M. Shepherd  
Charles A. Greer**

Sections of Neurobiology and Neurosurgery,  
Yale University School of Medicine,  
New Haven, Connecticut 06510, USA

## Cell damage by near-IR microbeams

SIR — Continuous-wave laser microbeams are generally used as diagnostic tools in laser scanning microscopes or, in the case of near-infrared microbeams, as optical traps for cell manipulation and force characterization<sup>1,2</sup>. Because single-beam traps are created with objectives of high numerical aperture (NA), typical trapping intensities and photon flux densities are, respectively, of the order of MW cm<sup>-2</sup> and 10<sup>27</sup> cm<sup>-2</sup> s<sup>-1</sup>. These extremely high fields may induce two-photon absorption processes<sup>3-5</sup> and anomalous biological effects.

We have investigated these phenomena by studying optically trapped motile human spermatozoa maintained in HEPES-buffered fresh human tubal fluid labelled with a live/dead fluorescence assay kit (Molecular Probes). Trapping effects at 760 and 800 nm (70 mW) were compared using a tunable, continuous-wave Ti:sapphire laser coupled to an inverted fluorescence microscope. Visible two-photon-excited intracellular fluorescence was detected with a cooled CCD camera.

Viable cells showed green fluores-

cence (515 nm) corresponding to the membrane-permeable live-cell probe SYBR 14 (Fig. 1). Damaged cells showed red fluorescence (636 nm), due to intranuclear accumulation of the membrane-impermeable dead-cell probe propidium iodide. Figure 1a shows a brightfield image illustrating sperm structure, flagellar motion and an intense green spot in the centre of the sperm head. Without brightfield illumination, the sub-micrometre spot persisted

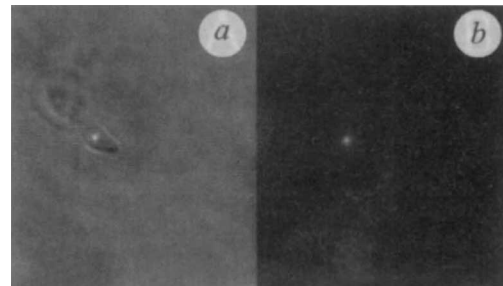


FIG. 1a, Brightfield image of a motile human sperm cell confined in the 760-nm optical trap. Two-photon-excited fluorescence of a live/dead fluorescent probe is clearly visible as an intense sub-micrometre spot in the 5- $\mu$ m-long sperm head despite the presence of halogen lamp illumination. b, The two-photon-excited fluorescent spot is more clearly visible in the absence of brightfield illumination.

- Chess, A., Simon, I., Cedar, H. & Axel, R. *Cell* **78**, 823-834 (1994).
- Lancet, D. A. *Rev. Neurosci.* **9**, 329-355 (1986).
- Ressler, K. J., Sullivan, S. L. & Buck, L. B. *Cell* **73**, 597-609 (1993).
- Vassar, R., Ngai, J. & Axel, R. *Cell* **74**, 309-318 (1993).
- Vassar, R. et al. *Cell* **79**, 981-991 (1994).
- Ressler, K. J., Sullivan, S. L. & Buck, L. B. *Cell* **79**, 1245-1255 (1994).
- Singer, M. S., Oliveira, L., Vriend, G. & Shepherd, G. M. *Receptors and Channels* (in the press).
- Singer, M. S. & Shepherd, G. M. *NeuroReport* **5**, 1297-1300 (1994).
- Kuipers, W. et al. in *Membrane Protein Models: Experiment, Theory and Speculation* (ed. Findlay, J.) (Oxford, BIOS, in the press).
- Hughes, A. L. & Hughes M. K. *J. molec. Evol.* **36**, 249-254 (1993).
- Engelman D. M., Steitz, T.A. & Goldman, A. A. *Rev. biophys. Chem.* **15**, 321-353 (1986).
- Buck, L. & Axel, R. *Cell* **65**, 175-187 (1991).
- Ben-Arie, N. et al. *Hum. molec. Genet.* **3**, 229-235 (1993).
- Strotmann, J., Wanner, I., Helfrich, T. & Breer, H. *Eur. J. Neurosci.* **7**, 492-500 (1995).
- Vriend, G. *J. molec. Graph.* **8**, 52-56 (1990).

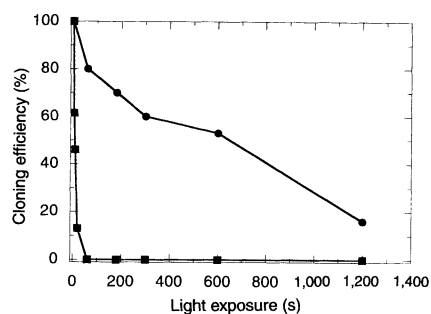


FIG. 2 Cloning efficiency against exposure time for CHO cells; 88 mW of 760-nm (■) and 800-nm (●) microirradiation.

and became red within  $65 \pm 21$  s ( $n=10$ ). This shows two effects of the 760-nm trapping beam. First, two-photon-excited visible fluorescence is induced by the near-infrared trapping beam. Second, green to red fluorescence changes (coinciding with cessation of flagellar motion at  $35 \pm 20$  s ( $n=10$ )) indicate that the trap can cause lethal damage. In contrast, we were able to maintain most sperm ( $96 \pm 6\%$ ,  $n=50$ ) in an 800-nm trap for 10 min without either loss in motility or intranuclear propidium iodide accumulation.

Unlabelled spermatozoa showed blue, two-photon-excited autofluorescence which became 10–100-fold brighter within 600 s of 760-nm trapping ( $n=10$ ). Autofluorescence was also detected during 800-nm trapping, but the spot intensity did not change. As autofluorescence signals are probably due to reduced pyridine coenzymes (NAD(P)H), 760-nm alterations may be a consequence of UVA-like, two-photon-induced perturbations of the cellular redox state (that is, oxidative stress).

A final indicator of cellular damage was provided by evaluating the cloning efficiency of microirradiated Chinese hamster ovary (CHO) cells. Interphase cells exposed for up to 1,200 s (88 mW) and maintained in an incubator for 5–6 days were considered to be unaffected by light if clones consisting of  $\geq 50$  cells were produced. Cells irradiated with 760 nm were unable to form clones following light exposures of  $\geq 60$  s, whereas cloning efficiencies of 80% and 50% were measured following 60- and 600-s exposures at 800 nm (Fig. 2).

In conclusion, continuous-wave near-infrared microbeams can stimulate multiphoton processes in single living cells. The consequences of microirradiation include

membrane permeability changes, alterations in cloning efficiency and UVA-like stress. These processes are clearly wavelength-dependent and should be considered during trapping experiments, particularly when using short-wavelength, near-infrared lasers.

**K. König\*, H. Liang  
M. W. Berns, B. J. Tromberg**

*Beckman Laser Institute and Medical Clinic,  
University of California, Irvine,  
Irvine, California 92715, USA*

## Kaposi's sarcoma in pregnant women

SIR — Lunardi-Iskandar *et al.*<sup>1</sup> demonstrated that the  $\beta$ -chain of human chorionic gonadotropin (hCG) kills Kaposi's sarcoma-derived cell lines in culture and inhibits tumour production by these cell lines in nude mice. They also observed regression of Kaposi's sarcoma in two women during pregnancy, when levels of this hormone are elevated<sup>2</sup>. Because of the potential aetiological and therapeutic significance of these results, we examined clinical data from the Dermatovenereology Clinic, University Teaching Hospital, Lusaka, Zambia. We postulated that if hCG protected against disease in humans, AIDS-related Kaposi's sarcoma would occur with lower frequency or severity during pregnancy.

We determined the pregnancy status of all female patients  $\leq 40$  years old who were newly diagnosed with AIDS-related Kaposi's sarcoma during 1994. For comparison, we used new cases of venereal ulcer or discharge presenting during 4 months (January, April, July and October) of that year. Non-pregnant women with Kaposi's sarcoma were further classified into those with and without a child under 2 years of age.

Thirteen (15%) of the 84 young women with Kaposi's sarcoma and 25 (19%) of the 133 young women with venereal disease were pregnant at the time of presentation. Adjusted for age, the odds ratio for the association of current pregnancy and Kaposi's sarcoma was 1.0 (95% confidence interval, 0.4–2.1). An additional 23 (27%) women with Kaposi's sarcoma had a child under 2 years of age. Thus, 36 (43%) of the Kaposi's sarcoma patients had been exposed to elevated levels of hCG within the past 2 years.

We also assessed the relationship of pregnancy status to extent of tumour at presentation, classified as localized against disseminated according to ref. 3. Seven (54%) of the 13 who were pregnant had disseminated disease, as compared with 12 (52%) of those with children under 2 years of age and 19 (40%) of the 48 who were neither pregnant nor had a

child under 2. The age-adjusted odds ratio for the association of current pregnancy and disseminated sarcoma was 1.3 (95% confidence interval, 0.4–4.2).

These clinical data do not support the prediction from laboratory results that hCG is protective against Kaposi's sarcoma. Our data are not adjusted for possible fertility differences between these patient groups, nor for possible referral bias due to pregnancy and/or antenatal care. Furthermore, lack of effect at physiological levels does not exclude efficacy at higher pharmacological levels, for which the best test is a randomized, controlled clinical trial. Nevertheless, as pregnant and non-pregnant women appear to have a similar risk of this disorder, it is likely that factors other than hCG explain the difference between men and women in incidence of Kaposi's sarcoma.

**Charles S. Rabkin**

*Viral Epidemiology Branch,  
National Cancer Institute, EPN/434,  
Bethesda, Maryland 20892, USA*

**George Chibwe, Kamuya Muyunda**

**Elizabeth Musaba**

*Dermatovenereology Clinic,  
University Teaching Hospital,  
Lusaka, Zambia*

SIR — The classical pregnancy hormone and tumour marker human chorionic gonadotropin (hCG) has long been known for its ability to sustain pregnancy. In addition, it acts as a survival factor by suppressing apoptotic cell death in reproductive organs<sup>4</sup>. An entirely adverse effect of hCG, its blocking ability on tumorigenesis and metastasis of Kaposi's sarcoma, has recently been reported<sup>1</sup>. The authors' hypothesis that the trophic hormone hCG and its free  $\beta$ -subunit ( $\beta$ hCG) cause regression of Kaposi's sarcoma was tested in immunodeficient Bg-nude mice as well as *in vitro* with pregnancy sera of human and mouse origin, and with different preparations of hCG-derived molecules. Their premises run contrary to several long-held concepts and definitions of endocrinology concerning the evolutionary origin, biological function and nomenclature of hCG-derived molecules.

From an evolutionary point of view, hCG is a young hormone, as the genetic events generating its  $\beta$ -subunit took place long after the lineages of rodents and primates diverged<sup>5</sup>. Rodents possess neither a  $\beta$ CG gene nor a placental hormone similar to CG (refs 6, 7). In consequence, the mouse displays a gestational profile of hormone dependency entirely distinct from humans. Human gestation is dependent on placental hCG right from the beginning, whereas for the maintenance of pregnancy in rodents pituitary-derived luteinizing hormone (LH) — the cognate molecule of hCG — is an indispensable stimulus only in the second trimester<sup>3</sup>. The question remains, what is causing the

\*Permanent address: Institute for Molecular Biotechnology, D-07708 Jena, Germany.

- Ashkin, A., Dziedzic, J. M., Bjorkholm, J. E. & Chu, S. *Opt. Lett.* **11**, 288–290 (1986).
- Svoboda, K. & Block, S. M. *A. Rev. Biophys. biomolec. Struct.* **23**, 247–285 (1994).
- Denk, W., Strickler, J. H. & Webb, W. W. *Science* **248**, 73–75 (1990).
- Kennedy, S. M. & Lytle, F. E. *Analyt. Chem.* **58**, 2643–2647 (1986).
- Hänninen, P. E., Soini, E. & Hell, S. W. *J. Microsc.* **176**, 222–225 (1994).